Time-resolved transport properties of a Y junction of Tomonaga-Luttinger liquid wires

Amit Agarwal*
Department of Physics, Indian Institute of Technology, Kanpur 208 016, India
(Received 5 July 2014; revised manuscript received 18 September 2014; published 4 November 2014)

We study time-resolved transport properties of a Y junction composed of interacting one-dimensional quantum wires using a bosonization approach. In particular, we investigate the ac conductivity of the Y junction formed from finite-length Tomonaga-Luttinger liquid wires based on a plasmon scattering approach for injected charge pulses of arbitrary shapes. In addition, we calculate the tunneling current and quantum noise of the Y junction arising from pointlike tunneling impurities at the junction, including finite-temperature effects. Our results will be useful for designing nanoelectronic quantum circuits and for interpreting time-resolved experiments [Kamata *et al.*, Nat. Nanotechnol. **9**, 177 (2014)] in interacting wires and their junctions.

DOI: 10.1103/PhysRevB.90.195403 PACS number(s): 73.23.−b, 73.63.Nm, 71.10.Pm

I. INTRODUCTION

One-dimensional (1D) quantum wires and the junctions of several 1D quantum wires are expected to be important for potential applications as components in future nanoelectronic devices. Such 1D quantum wires with interacting electrons are described by the Tomonaga-Luttinger liquid (TLL) theory [1–6], the low-energy excitations in which are the collective density oscillations. These density oscillations or plasmon modes are markedly different from their counterparts, i.e., Landau's quasiparticle excitations, in higher dimensions described very successfully by the Fermi liquid (FL) theory [7]. This leads to unique physics in 1D, such as the spin-charge separation in which the spin and charge excitations propagate with different velocities [8,9], or the phenomena of charge fractionalization [10–12]. Recently, charge fractionalization has also been observed using time-resolved measurements on coupled integer quantum Hall edge channels [13].

In the present work, we investigate the time-dependent transport properties of multiwire junctions, and a three-wire Y junction in particular. These have already been realized experimentally in crossed single-walled carbon nanotubes [14,15]. Such Y junctions with interacting quantum wires are also extremely "rich" from a basic physics viewpoint and continue to be explored very actively in the literature [16–31]. Earlier theoretical studies of Y junctions have primarily focused on the fixed points of the junction, their stability analysis, and the associated dc conductivity. These studies either use the fermionic language and the weak-interaction renormalization-group (RG) approach [17], the bosonic and conformal field theory language [19,21], or other numerical methods such as the functional RG [20]. A comprehensive study of the fixed points of the Y junction formed from spinless interacting electrons, and the dc conductance, was carried out in Ref. [19]. This was later extended to include spinful electrons giving a much richer phase diagram in the parameter space of charge and spin interactions [24], and to account for different interaction strengths in different wires [30].

Time-dependent transport properties of 1D TLL wires have also been studied earlier. Quantum noise for an infinite TLL wire with pointlike tunneling impurity, around the "connected" fixed point of a two-wire junction, was studied in Ref. [32]. The ac conductivity of a clean finite-length TLL wire was calculated in Refs. [10,33]. This has been recently generalized to include arbitrary wave-packet shapes of the incident current in Ref. [34]. Comparatively, the time-dependent transport properties of Y junctions have drawn much less attention in the literature and it is the aim of this paper to rectify this.

In this paper, we study the ac conductivity, the tunneling current, and quantum noise (including shot noise and Josephson noise) of a Y junction tuned to a dissipationless fixed point with spinless TLL wires. We consider both time-reversal symmetry (TRS)-preserving and TRS-violating junctions and use the single-parameter description of the dissipationless fixed points of the junction given in Refs. [21,26]. Our analysis may be useful for interpreting time-resolved experiments [13] in multiwire junctions and for designing nanoelectronic quantum circuits [35].

This paper is organized as follows. In Sec. II, we discuss the details of the three-wire Y junction and show that both the Coulomb interactions in the wire and the "scattering" boundary conditions at the junction can be treated using bosonization with delayed evaluation of the boundary conditions [19]. In Sec. III, we calculate the ac conductivity of the Y junction formed from finite-length TLL wires which are connected to FL leads—see Fig. 1(a). We also reproduce the known results for a two-wire junction, and the dc conductivity as a limiting case of our calculations. In Sec. IV, we calculate the tunneling current and quantum noise at the junction with infinite TLL wires [see Fig. 1(b)], in the presence of pointlike tunneling impurities at the Y junction tuned to a dissipationless fixed point. Finally, we summarize our findings in Sec. V.

II. BOSONIZATION OF THE JUNCTION—DELAYED EVALUATION OF THE BOUNDARY CONDITION

In this section, we review the technique of bosonization for the wire and, subsequently, the parametrization of the dissipationless fixed points at the junction.

A. Bosonization of the wires

To model a junction of multiple wires, let us assume that N semi-infinite wires meet at a junction. The wires are modeled as spinless TLL on a half line and are parametrized by coordinates

*amitag@iitk.ac.in

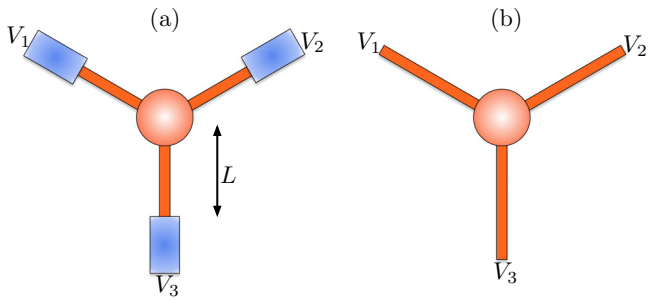

FIG. 1. (Color online) Schematic of a Y junction composed of TLL wires. (a) A Y junction of finite-length TLL wires (red) connected to Fermi-liquid leads at the ends (blue) with different applied voltages. (b) A Y junction of infinite TLL wires.

x_i, $i = 1,2,\ldots,N$, such that $x_i > 0$. We use a folded basis to describe the junction, i.e., we choose a convention that for all the wires, $x_i = 0$ at the junction and x_i increases from 0 as one goes outwards from the wires. We denote the incoming and outgoing single-electron wave functions on wire i by $\phi_{i\mathrm{I}}$ and $\phi_{i\mathrm{O}}$, respectively, which in turn are proportional to plane waves $\exp[-ik(x_i + vt)]$ and $\exp[ik(x_i - vt)]$, respectively, for a given wave number $k > 0$ and velocity v. For simplicity of analysis, we consider all the semi-infinite spinless TLL wires to have the same short-range electron-electron (e-e) interaction strength and Fermi velocity.

The spinless electron field on each wire can be expressed as $\psi(x) = \psi_{\mathrm{I}}(x) + \psi_{\mathrm{O}}(x)$ where the incoming/outgoing fermionic fields $\psi_{\mathrm{I/O}}$ can be bosonized [5] as

$$\psi_{\mathrm{I}}(x) = \frac{1}{\sqrt{2\pi\alpha}} F_{\mathrm{I}} e^{2i\pi N_{\mathrm{I}}(x+vt)/L} e^{-ik_{\mathrm{F}}x + i\phi_{\mathrm{I}}(x)},$$
$$\psi_{\mathrm{O}}(x) = \frac{1}{\sqrt{2\pi\alpha}} F_{\mathrm{O}} e^{2i\pi N_{\mathrm{O}}(x-vt)/L} e^{ik_{\mathrm{F}}x + i\phi_{\mathrm{O}}(x)}. \quad (1)$$

Here, F_{I} and F_{O} are Klein factors for the incoming and outgoing electrons, respectively, k_{F} is the Fermi momentum, and α is the inverse ultraviolet (short-distance) cutoff. N_{I} and N_{O} count the number of incoming and outgoing chiral particles with respect to the filled Fermi sea. The fields $\phi_{\mathrm{I}}(x)$ and $\phi_{\mathrm{O}}(x)$ are the incoming (left-moving) and the outgoing (right-moving) chiral bosonic fields in each wire and can be expressed in terms of the bosonic creation and destruction operators as

$$\phi_{\mathrm{O/I}} \equiv \sum_{q>0} \frac{1}{\sqrt{n_q}} (b_{q\mathrm{O/I}} e^{\pm iqx} + b^{\dagger}_{q\mathrm{O/I}} e^{\mp iqx}) e^{-\alpha|q|/2}. \quad (2)$$

The Lagrangian of the system is given by $\mathcal{L} = \mathcal{L}_0 + \mathcal{L}_{\mathrm{int}}$, where $\mathcal{L}_0$ describes free electrons in the wire, and is given by

$$\mathcal{L}_0 = \frac{1}{4\pi} \sum_{i=1}^{N} \int_0^L dx [\partial_x \phi_{i\mathrm{O}} (-\partial_t - v\partial_x)\phi_{i\mathrm{O}} + \partial_x \phi_{i\mathrm{I}} (\partial_t - v\partial_x)\phi_{i\mathrm{I}})], \quad (3)$$

where v denotes the Fermi velocity which we take to be same in all the wires and i is the wire index. The corresponding incoming and outgoing density and current fields in each wire are given by

$$\rho_{i\mathrm{O}} = \frac{\partial_x \phi_{i\mathrm{O}}}{2\pi} + \frac{N_{i\mathrm{O}}}{L}, \quad J_{i\mathrm{O}} = -\frac{\partial_t \phi_{i\mathrm{O}}}{2\pi} - \frac{N_{i\mathrm{O}}}{L},$$
$$\rho_{i\mathrm{I}} = -\frac{\partial_x \phi_{i\mathrm{I}}}{2\pi} + \frac{N_{i\mathrm{I}}}{L}, \quad J_{i\mathrm{I}} = \frac{\partial_t \phi_{i\mathrm{I}}}{2\pi} - \frac{N_{i\mathrm{I}}}{L}. \quad (4)$$

We emphasize here that the second term in the expressions for density and current arise from an excessive number of incoming and outgoing fermions with respect to the ground state (filled Fermi sea), and can be controlled by applying an external dc voltage in each TLL wire. These terms will be very useful in Sec. IV, where we apply different dc bias voltage on each of the three wires. However, for calculating the ac conductivity in Sec. III, only the first term of the current expression (temporal derivative of the fluctuating fields) is needed since the average dc voltage is zero in all the wires, and we will use the notation

$$j_{i\mathrm{O}} = -\frac{\partial_t \phi_{i\mathrm{O}}}{2\pi} \quad \text{and} \quad j_{i\mathrm{I}} = \frac{\partial_t \phi_{i\mathrm{I}}}{2\pi}, \quad (5)$$

in Sec. III.

For a short-range e-e interaction between the two chiral modes in the wire, the term in the Lagrangian for each wire i is of the form

$$\mathcal{L}^i_{\mathrm{int}} = \frac{\lambda}{4\pi} \int_0^L dx \partial_x \phi_{i\mathrm{I}} \partial_x \phi_{i\mathrm{O}}, \quad (6)$$

where λ is the e-e interaction strength (positive for repulsive interactions) with the dimensions of velocity. Note that for each of the wires described by Eqs. (3) and (6), the effective TLL velocity and the effective TLL interaction strength are given by

$$\tilde{v} = \sqrt{v^2 - \lambda^2/4}, \quad \text{and} \quad g = \sqrt{\frac{v - \lambda/2}{v + \lambda/2}}. \quad (7)$$

B. Bosonization of the junction

To describe the junction uniquely, we need to impose an appropriate boundary condition on the fields at the junction, i.e., at $x = 0$. Following standard procedure [19,21,26], the incoming and outgoing currents and, consequently, the bosonic fields are related at the junction by a current splitting matrix $\mathbb{M}$, i.e., $j_{\mathrm{O}i} = \sum_j \mathbb{M}_{ij} j_{\mathrm{I}j}$, which leads to $\phi_{\mathrm{O}i} = \sum_j \mathbb{M}_{ij} \phi_{\mathrm{I}j}$. Here we have ignored an integration constant which plays no (physical) role in the computation of the Green's functions of the fields and, consequently, on the scaling dimensions of various operators. In order to ensure that the matrix $\mathbb{M}$ represents a fixed point of the theory, the incoming and outgoing fields must satisfy appropriate bosonic commutation relations; this restricts the matrix $\mathbb{M}$ to be orthogonal. Scale invariance or conformal invariance imposes the same constraints of orthogonality [25] on $\mathbb{M}$. The constraint of orthogonality also implies that there is no dissipation in the system [36]. In addition, to ensure current conservation at the junction, its rows (or columns) have to add up to unity.

Since ϕ_{O} and ϕ_{I} are interacting fields, we need to perform a Bogoliubov transformation on them,

$$\phi_{\mathrm{O/I}} = \frac{1}{2\sqrt{g}} [(1+g)\tilde{\phi}_{\mathrm{O/I}} + (1-g)\tilde{\phi}_{\mathrm{I/O}}], \quad (8)$$

to obtain the corresponding "free" outgoing and incoming ($\tilde{\phi}_{O/I}$) chiral fields, which satisfy the "free" field commutation relations: $[\tilde{\phi}_{O/I}(x,t),\tilde{\phi}_{O/I}(x',t)] = \pm i\pi\,\mathrm{sign}(x-x')$, where the sign function is defined as $\mathrm{sign}(x) = 1,0,-1$ for $x > 0$, $x = 0$, and $x < 0$, respectively. However, unlike the usual Bogoliubov transformation in the bulk, here we also need to consider the effect of the junction matrix $\mathbb{M}$ relating the interacting incoming and outgoing fields [21], which leads to a "Bogoliubov transformation" of the matrix: $\mathbb{M} \to \widetilde{\mathbb{M}}$. Qualitatively, $\mathbb{M}$ is related to tunnelings between the different wires and tunneling in each wire, at a dissipationless junction. The Bogoliubov transformed matrix $\widetilde{\mathbb{M}}$ which relates the free incoming and outgoing fields, $\tilde{\phi}_{Oi}(x) = \sum_j \widetilde{\mathbb{M}}_{ij}\tilde{\phi}_{Ij}(-x)$, is given by

$$\widetilde{\mathbb{M}} = [(1+g)\mathbb{I} - (1-g)\mathbb{M}]^{-1}[(1+g)\mathbb{M} - (1-g)\mathbb{I}]. \quad (9)$$

We emphasize that this description is valid for a dissipationless junction of any number of interacting one-dimensional wires.

For the case of a two-wire junction, there are only two classes of orthogonal matrices: a rotation matrix whose determinant is 1 and a reflection matrix whose determinant is -1. The constraint that the columns (or rows) add up to one implies that there is only one matrix in each class. These are given by

$$\begin{pmatrix} 1 & 0 \\ 0 & 1 \end{pmatrix} \quad \text{and} \quad \begin{pmatrix} 0 & 1 \\ 1 & 0 \end{pmatrix}, \quad (10)$$

which corresponds to the cases of the "disconnected" and the "connected" fixed points of a two-wire junction, respectively. In what follows, we focus on a three-wire Y junction.

A detailed study of the three-wire spinless TLL junction using bosonization and boundary conformal field theory can be found in Refs. [19,25]. In particular, for a three-wire charge-conserving junction, all current splitting orthogonal matrices $\mathbb{M}$ whose rows add up to one can be parametrized by a single continuous parameter θ, and are divided into two classes on the basis of TRS: $\det \mathbb{M}_1 = 1$, and $\det \mathbb{M}_2 = -1$. These two classes of matrices are explicitly given by

$$\mathbb{M}_1 = \begin{pmatrix} a & b & c \\ c & a & b \\ b & c & a \end{pmatrix}, \quad \mathbb{M}_2 = \begin{pmatrix} b & a & c \\ a & c & b \\ c & b & a \end{pmatrix}, \quad (11)$$

where $a = (1+2\cos\theta)/3$, $b = (1-\cos\theta+\sqrt{3}\sin\theta)/3$, and $c = (1-\cos\theta-\sqrt{3}\sin\theta)/3$. This gives us an explicit single-parameter characterization of the two families of fixed points; any fixed point in the theory can now be identified in terms of θ, with the fixed points at $\theta = 0$ and $\theta = 2\pi$ being identical.

Note that the current splitting matrix $\mathbb{M}$ preserves TRS, only if it is symmetric. Thus the junction current splitting matrices belonging to the $\mathbb{M}_2$ class represent an asymmetric class (in wire indices) of fixed points for systems with TRS. The $\mathbb{M}_1$ class represents a Z_3 symmetric (in the wire index) class of fixed points and generally denotes systems with broken TRS, which can arise, for instance, due to a magnetic field at the junction (assuming a finite cross-sectional area). In the $\mathbb{M}_1$ class of fixed points, only two points given by $\theta = 0,\pi$, at which the asymmetry producing $\sin\theta$ term vanishes, are TRS invariant. For the $\mathbb{M}_1$ class, $\theta = \pi$, or $[a,b,c] = [-1/3,2/3,2/3]$, corresponds to the so-called Dirichlet fixed point (D_P). The disconnected fixed point (N), where there is no tunneling between any pair of wires, is given by $\theta = 0$ (i.e., $[a,b,c] = [1,0,0]$). The cases of $\theta = 2\pi/3$ (i.e., $[a,b,c] = [0,1,0]$) and $4\pi/3$ correspond to the chiral χ_- and χ_+ fixed points, respectively, following the notation of Ref. [19].

Note that the $\mathbb{M}_2$ class of fixed-point matrices has the interesting property that $(\mathbb{M}_2)^2 = \mathbb{I}$. As a consequence, $\widetilde{\mathbb{M}}_2 = \mathbb{M}_2$, which implies that both the interacting and the free fields satisfy identical boundary conditions at the junction. This is not true for the $\mathbb{M}_1$ class of fixed-point matrices, but the matrix $\widetilde{\mathbb{M}}_1$ still has the same form as the matrix $\mathbb{M}_1$ with the corresponding parameters given by $\tilde{a} = [3g^2 - 1 + (3g^2+1)\cos\theta]/\delta$ and $\tilde{b}/\tilde{c} = 2(1-\cos\theta \pm \sqrt{3}g\sin\theta)/\delta$, where $\delta = 3[1+g^2+(g^2-1)\cos\theta]$. Note that the matrices $\widetilde{\mathbb{M}}_1$ are nonlinear functions of the TLL parameter g, while the matrices $\widetilde{\mathbb{M}}_2$ are independent of g. This will have nontrivial manifestations for physical observables (e.g., quantum noise, tunneling current, etc.—see Sec. IV), when we consider a junction slightly away from the fixed points, as scaling dimensions of operators switched on perturbatively around the $\mathbb{M}_1$ class will generally be nonlinear functions of g. On the other hand, for the $\mathbb{M}_2$ class of fixed points, the scaling dimensions of operators will always be linear functions of g.

Having characterized the junction, we now proceed to study the ac conductivity of a Y junction formed from finite-length TLL wires, connected to FL leads—see Fig. 1(a).

III. AC CONDUCTIVITY

In this section, we consider an incident charge wave packet originating in the FL lead connected to one of the TLL wires, say i, and its consequent motion after undergoing charge fractionalization at the FL-TLL boundaries and at the junction. This will also allow us to calculate the low-frequency ac current splitting matrix $\mathbb{S}$, which relates the complex amplitudes of the incoming ac currents to the complex amplitudes of the outgoing current, in the linear response regime. Such a time-resolved measurement of an incident wave packet in a TLL wire of integer quantum Hall edge channels was recently used to identify a single-charge fractionalization event [13]. In our language, this corresponds to a two-wire junction tuned to be at the "connected" fixed point (effectively a single finite-length TLL wire connected to FL leads).

In the dc limit, i.e., $\omega \to 0$, all signatures of charge fractionalization are lost and $\mathbb{S} \to \mathbb{M}$, which is the noninteracting current splitting matrix for a junction with finite TLL wires connected to the FL leads [Fig. 1(a)]. For a junction with TLL wires extending to infinity, it simply reduces to the interacting current splitting matrix at the junction for all frequencies, $\mathbb{S} \to \widetilde{\mathbb{M}}$, since there is no FL-TLL interface. However, for finite-length wires at finite frequencies, $\mathbb{S}$ depends on the fixed point, the strength of the e-e interaction, and the length of the TLL wires L, and it carries the signature of charge fractionalization events at the FL-TLL boundary.

In our model of the junction, there is no mechanism of power dissipation. Thus the average over one oscillation cycle of the incoming energy must be equal to the average outgoing

energy per cycle. This imposes the constraint of unitarity on the $\mathbb{S}$ matrix, which also serves as a useful check for our calculations. Also note that we are considering all three wires to have the same Fermi velocity and *e*-*e* interaction strengths, and these are connected at the junction described by boundary conditions which are cyclic in nature. Thus we expect to have only a few independent coefficients in $\mathbb{S}$, which should also appear in a cyclic manner.

Before discussing the solution of the generalized plasmon scattering problem [34] at the junction, we emphasize that this calculation is valid only in the linear response regime and only for ac frequencies which do not breach the linearization regime for each TLL wire, i.e., $\omega < v/\alpha$. Also note again that we use a folded basis for describing the junction such that all the wires go from $x = 0$ to $x = \infty$ and the junction lies at $x = 0$.

The time evolution of the "injected" wave packet is given by the coupled equation of motion (EOM) for the expectation value of the incoming ($\phi_{i\mathrm{I}}$) and outgoing ($\phi_{i\mathrm{O}}$) fields in wire i, which are governed by the Lagrangian given in Eqs. (3) and (6). The EOM are

$$\partial_x\left[\partial_t\phi_{i\mathrm{I}} - v\partial_x\phi_{i\mathrm{I}} + \frac{\lambda}{2}\partial_x\phi_{i\mathrm{O}}\right] = 0, \tag{12}$$

$$\partial_x\left[\partial_t\phi_{i\mathrm{O}} + v\partial_x\phi_{i\mathrm{O}} - \frac{\lambda}{2}\partial_x\phi_{i\mathrm{I}}\right] = 0. \tag{13}$$

Let us now consider an electronic wave packet incident on TLL wire i from the FL lead. The incoming bosonic field $\phi_{\mathrm{I}}(x,t)$ in the FL lead ($x > L$) can be expressed in terms of scattering states of energy $\omega = vq$ by the following relation:

$$\phi_{i\mathrm{I}}(x,t) = \int_{-\infty}^{\infty}\frac{dq}{2\pi}\phi_{i\mathrm{I}}(q)e^{-i[q(x-L)+\omega t]}. \tag{14}$$

Here, $\phi_{i\mathrm{I}}(q)$ is specified by the Fourier transform $\rho_{i\mathrm{I}}(q)$ of the incident charge density in wire i, $\rho_{i\mathrm{I}}(x,t=0)$, by the relation $\phi_{i\mathrm{I}}(q) = \frac{2\pi}{iq}\rho_{i\mathrm{I}}(q)$—see Eq. (4). The extra factor of e^{iqL} in the above equation just shifts the position of the origin of the axis in the FL leads, and it simplifies the calculations below. The outgoing bosonic scattering state in the FL lead of wire j due to in injected state in wire i only is given by

$$\phi^{(i)}_{j\mathrm{O}}(x,t) = \int_{-\infty}^{\infty}\frac{dq}{2\pi}\phi^{(i)}_{j\mathrm{O}}(q)e^{i[q(x-L)-\omega t]}, \tag{15}$$

where the outgoing amplitude in the momentum space is related to the incoming amplitude via the elements of the ac current splitting matrix:

$$\phi^{(i)}_{j\mathrm{O}}(q) = s_{ji}(q)\phi_{i\mathrm{I}}(q), \tag{16}$$

with s_{ji} denoting the matrix elements of $\mathbb{S}$ and $q = \omega/v$. We emphasize here that we are considering all the wires to have the same Fermi velocity. In the case of the bosonic states being incident in all the wires, the total outgoing bosonic field gets contribution from all the incoming fields and it is explicitly given by $\phi_{j\mathrm{O}}(x,t) = \sum\phi^{(i)}_{j\mathrm{O}}(x,t)$ or, equivalently,

$$\phi_{j\mathrm{O}}(x,t) = \sum_i\int_{-\infty}^{\infty}\frac{dq}{2\pi}s_{ji}(q)\phi_{i\mathrm{I}}(q)e^{i[q(x-L)-\omega t]}. \tag{17}$$

If the elements s_{ij} of $\mathbb{S}$ are known, then the total time-dependent density ($\rho = \rho_{\mathrm{I}} + \rho_{\mathrm{O}}$) and the total outgoing current ($j = j_{\mathrm{I}} + j_{\mathrm{O}}$) in the FL of wire j, due to an incoming wave packet in wire i, is given by

$$\rho^{(i)}_j(x,t) = \int_{-\infty}^{\infty}\frac{dq}{2\pi}\rho_{i\mathrm{I}}(q)e^{-i\omega t}[e^{-iq(x-L)}\delta_{ij} + s_{ji}e^{iq(x-L)}], \tag{18}$$

and

$$j^{(i)}_j(x,t) = v\int_{-\infty}^{\infty}\frac{dq}{2\pi}\rho_{i\mathrm{I}}(q)e^{-i\omega t}[-e^{-iq(x-L)}\delta_{ij} + s_{ji}e^{iq(x-L)}]. \tag{19}$$

In the TLL wire region ($x < L$), the incoming and outgoing fields, corresponding to a situation when there is only an incoming field in wire i, are given by

$$\phi^{(i)}_{j\frac{\mathrm{I}}{\mathrm{O}}}(x,t) = \int_{-\infty}^{\infty}\frac{dq}{2\pi}\phi_{i\mathrm{I}}(q)e^{-i\omega t}\left(a^{(i)}_{j\frac{\mathrm{I}}{\mathrm{O}}}e^{-ikx} + b^{(i)}_{j\frac{\mathrm{I}}{\mathrm{O}}}e^{ikx}\right). \tag{20}$$

Here the ac frequency $\omega = \tilde{v}k$, where $\tilde{v}$ is the renormalized Fermi velocity in the TLL region and is given by Eq. (7). Note that in Eq. (20) above, q is the wave vector in the noninteracting FL leads, and k denotes the wave vector in the interacting TLL region for the fixed incoming energy ω and they are related to each other via the equation $k = vq/\tilde{v}$.

We now proceed to solve the "plasmon scattering" problem and obtain the elements of $\mathbb{S}$. Let us consider an incoming current (from FL lead) only in wire 1. The continuity of the incoming and the outgoing currents at $x = L$ [using Eqs. (14), (15), and Eq. (20), in Eq. (5)] gives the following equations in each wire (six in all):

$$a^{(1)}_{i\mathrm{I}}e^{-ikL} + b^{(1)}_{i\mathrm{I}}e^{ikL} = \delta_{i1}, \tag{21}$$

$$a^{(1)}_{i\mathrm{O}}e^{-ikL} + b^{(1)}_{i\mathrm{O}}e^{ikL} = s_{i1}, \tag{22}$$

where s_{i1} are the elements of the first column of $\mathbb{S}$, and the superscript is used to indicate that the incoming current is in wire 1. Within the TLL region ($x < L$), substituting Eq. (20) in Eqs. (12) and (13) gives the following set of equations for each wire (six in all):

$$2(\omega - vk)a^{(1)}_{i\mathrm{I}} + k\lambda a^{(1)}_{i\mathrm{O}} = 0, \tag{23}$$

$$2(\omega - vk)b^{(1)}_{i\mathrm{I}} - k\lambda b^{(1)}_{i\mathrm{O}} = 0, \tag{24}$$

in addition to the consistency condition $\omega = \tilde{v}k$, with $\tilde{v} = \sqrt{v^2 - \lambda^2/4}$. Besides these, the boundary condition at the junction ($x = 0$) is given by the field (current) splitting matrix $\mathbb{M}$ as

$$a^{(1)}_{i\mathrm{O}} + b^{(1)}_{i\mathrm{O}} = \sum_j\mathbb{M}_{ij}\left(a^{(1)}_{j\mathrm{I}} + b^{(1)}_{j\mathrm{I}}\right). \tag{25}$$

Solving these 15 equations simultaneously gives us the three elements of the first column of the ac current splitting matrix. Repeating this calculation for the case with an incoming unit current in the other wires will give us the elements in the other two columns.

A. TRS-preserving ($\mathbb{M}_2$) fixed points

Let us first consider the TRS-preserving systems, i.e., Y junctions with the $\mathbb{M}_2$ class of fixed points. Following the procedure described above, we calculate the ac current splitting matrix $\mathbb{S}$, which has only six independent components. These are are given by

$$s_{11} = \frac{1}{\xi}[2\tilde{v}b - i\lambda \sin(2kL)], \tag{26}$$

$$s_{22} = \frac{1}{\xi}[2\tilde{v}c - i\lambda \sin(2kL)], \tag{27}$$

$$s_{33} = \frac{1}{\xi}[2\tilde{v}a - i\lambda \sin(2kL)], \tag{28}$$

$$s_{21} = \frac{2}{\xi}\tilde{v}a, \tag{29}$$

$$s_{31} = \frac{2}{\xi}\tilde{v}c, \tag{30}$$

$$s_{32} = \frac{2}{\xi}\tilde{v}b, \tag{31}$$

where a, b, and c are defined below Eq. (11), and, finally,

$$\xi = 2[\tilde{v}\cos(2kL) - iv\sin(2kL)]. \tag{32}$$

We note again that the ω dependence of $\mathbb{S}$ appears in Eqs. (26)–(32) via k which is defined after Eq. (24).

The other elements of $\mathbb{S}$ are given by $s_{12} = s_{21}$,$s_{13} = s_{31}$, and, finally, $s_{23} = s_{32}$. Note that the three off-diagonal elements and the three diagonal elements have a very similar structure and differ only due to the different corresponding element in the current splitting matrix $\mathbb{M}_2$ at the junction.

To get some physical insight for the form of $\mathbb{S}$, let us consider the specific case of a junction with $\theta = 0$ in the $\mathbb{M}_2$ class, i.e., $[a,b,c] = [1,0,0]$, which parameterizes the case of wires 1 and 2 being directly connected, effectively becoming one wire of length $2L$, and wire 3 being completely disconnected from the other two. For this case, Eqs. (26) and (29) reduce to

$$s_{11} = \frac{-i(\lambda/2)\sin 2kL}{\tilde{v}\cos(2kL) - iv\sin(2kL)}, \tag{33}$$

$$s_{21} = \frac{\tilde{v}}{\tilde{v}\cos(2kL) - iv\sin(2kL)}. \tag{34}$$

As a check of our calculations, we note that Eqs. (33) and (34) are identical to the set of equations given in Eq. (17) of Ref. [37], which were derived for counterpropagating quantum Hall edge states which interact with each other. Furthermore, this simpler case can also be derived by considering a steplike variation of the interaction strength, i.e., $g(x) = g$ for $-L < x < L$, and $g(x) = 1$ otherwise, in an interacting 1D wire [10,33]. Consider an electronic wave-packet incident on the interacting region from the noninteracting region. Fractionalization of charge [11] in the interacting region implies the reflection of fractional charge $q^* = r_0 e$, where $r_0 = (1-g)/(1+g)$ and transmission of a fractional charge $q^* = t_0 e$ into the interacting region, where $t_0 = 2g/(1+g)$. Other reflection and transmission coefficients for a single impact are given by $r_0' = -r_0$, and $t_0' = 2/(1+g)$. The overall reflection and transmission probability in this case can be obtained by considering the infinite sequence of reflection and transmission from the two boundaries of the finite-length interacting region, and are given by

$$r(\omega) = r_0 + t_0 t_0' \sum_{n=1}^{\infty} (r_0' e^{2i\omega L/\tilde{v}})^{2n} = r_0 \frac{1 - e^{4i\omega L/\tilde{v}}}{1 - r_0^2 e^{4i\omega L/\tilde{v}}}, \tag{35}$$

which is identical to Eq. (33). Note that $r_0 = \lambda/2(v+\tilde{v})$. The overall transmission coefficient is given by the sum of the following infinite series:

$$t(\omega) = t_0 t_0' e^{2i\omega L/\tilde{v}} \sum_{n=0}^{\infty} (r_0' e^{2i\omega L/\tilde{v}})^{2n} = \frac{t_0 t_0' e^{2i\omega L/\tilde{v}}}{1 - r_0^2 e^{4i\omega L/\tilde{v}}}, \tag{36}$$

and is identical to Eq. (34).

We thus see that the ac scattering coefficients encode the full history of the trajectory of the electron including multiple-charge fractionalization events at the FL-TLL interfaces, and at the junction.

B. TRS-violating ($\mathbb{M}_1$) fixed points

We now consider the case of Y junctions which do not preserve TRS, i.e., the $\mathbb{M}_1$ class of fixed points. In this case, the $\mathbb{S}$ matrix has the same cyclic form of the $\mathbb{M}_1$ class of matrices and it has only three independent elements, since all the diagonal elements of $\mathbb{M}_1$ are identical. Following the same procedure as in the previous case, we calculate the elements of $\mathbb{S}$ to be

$$\begin{aligned} s_{11} = \lambda^{-1}\eta^{-1}[&\tilde{v}(8\tilde{v}\{2\tilde{v}e^{3ikL}\cos(kL)[2\lambda\cos\theta + 3\cos(2kL) \\ &\times(-2\lambda\cos\theta - \lambda + 4v) + \lambda - 12v] - 3\tilde{v}^2(-1 + e^{2ikL}) \\ &\times(1+e^{2ikL})^2 + ie^{3ikL}\sin(kL)[3\lambda(2\cos\theta + 1)(2v - \lambda) \\ &\times \cos(2kL) - 2\lambda\cos\theta(2v+\lambda) + (6v + \lambda)(4v - \lambda)]\} \\ &- 3(-1 + e^{2ikL})^2(1 + e^{2ikL})(\lambda^3 + 16v^3 - 8\lambda v^2\cos\theta \\ &- 4\lambda v^2)) + 3v(-1 + e^{2ikL})^3(2v - \lambda)(\lambda^2 \\ &+ 4v^2 - 4\lambda v\cos\theta)], \end{aligned} \tag{37}$$

where

$$\begin{aligned} \eta = 12e^{3ikL}&[2\zeta - \lambda\sin(kL)]\{[2\zeta - \lambda\sin(kL)]^2 \\ &+ 4i\lambda\sin(kL)\zeta(1 - \cos\theta)\} \end{aligned} \tag{38}$$

and

$$\zeta = \tilde{v}\cos(kL) - iv\sin(kL). \tag{39}$$

The other elements of $\mathbb{S}$ are given by

$$s_{21} = -48\eta^{-1}\tilde{v}^2 e^{3ikL}[2\zeta c - i\lambda\sin(kL)b], \tag{40}$$

$$s_{31} = 48\eta^{-1}\tilde{v}^2 e^{3ikL}[2\zeta^* c + i\lambda\sin(kL)b], \tag{41}$$

along with $s_{22} = s_{33} = s_{11}$,$s_{12} = s_{23} = s_{31}$, and, finally, $s_{13} = s_{32} = s_{21}$.

In Fig. 2, we plot the absolute values of some of the elements of $\mathbb{S}$, as a function of the incoming energy ($\omega = \tilde{v}k$) and the parameter θ describing the fixed points of the junction. Note that unlike the dc conductivity, the ac current amplitudes carry signatures of the e-e interactions, i.e., they depend on the e-e

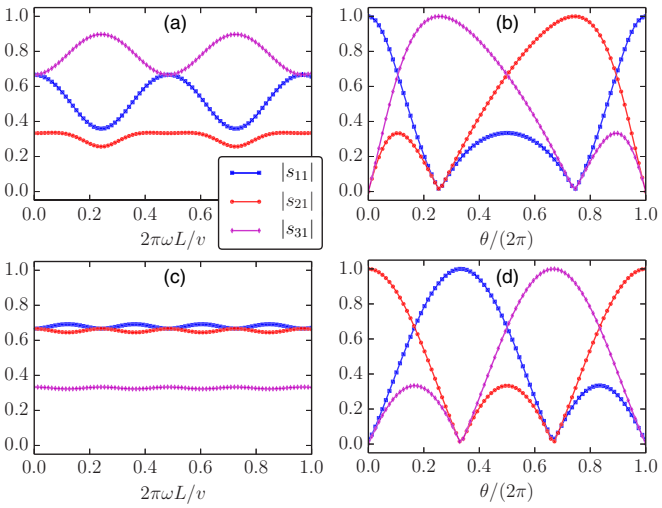

FIG. 2. (Color online) The amplitudes of the ac current splitting matrix for (a) the $\mathbb{M}_1$ class as a function of the frequency ω at the fixed point parameterized by $\theta = \pi/3$, (b) the $\mathbb{M}_1$ class as a function of θ for $\omega L/v = \pi/2$, (c) the $\mathbb{M}_2$ class as a function of ω with $\theta = \pi/3$, and (d) the $\mathbb{M}_2$ class as a function of θ for $\omega L/v = \pi/2$. The curves marked by blue squares, red circles, and magenta diamonds represent $|s_{11}|, |s_{21}|, |s_{31}|$, respectively, in all of the panels. The *e-e* interaction strength is chosen to be $\lambda = 0.5v$ (which gives $\tilde{v} = 0.97v$ and $g = 0.88$).

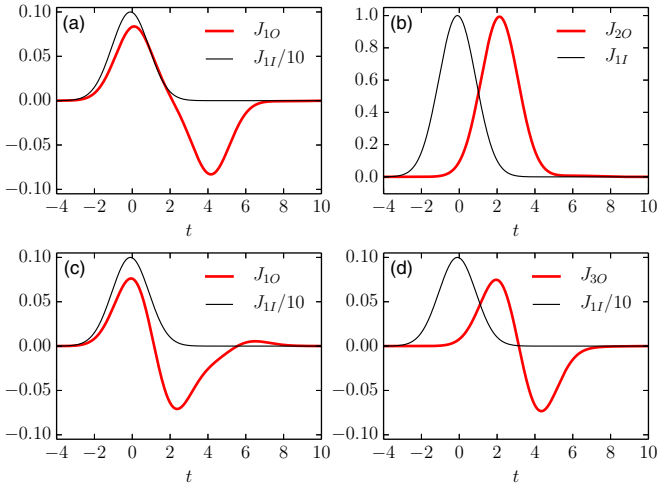

FIG. 3. (Color online) Pulse propagation in a Y junction as a function of time, for an incoming current only in wire 1. For the junction tuned to $\theta = 0$ fixed point of class $\mathbb{M}_2$, (a) shows the outgoing reflected current in wire 1 and (b) shows the outgoing transmitted current in wire 2. In this case, wires 1 and 2 are completely connected, effectively becoming one wire, and wire 3 is completely disconnected. For the junction tuned to the chiral fixed point χ_+, i.e., $\theta = 4\pi/3$ of the $\mathbb{M}_1$ class of fixed points, (c) shows the outgoing (reflected) current in wire 1 and (b) shows the outgoing (transmitted) current in wire 3.

interaction strength λ and the finite length L of the TLL wires. The amplitudes oscillate as a function of the frequency of the incident ac current with a period of $2\pi\tilde{v}/L$ for the $\mathbb{M}_1$ class of fixed points and with a period of $\pi\tilde{v}/L$ for the $\mathbb{M}_2$ class of fixed points, as can be seen from Figs. 2(a) and 2(c), respectively. Experimentally, such measurements of oscillations of the ac current amplitude as a function of the frequency may be used to classify the Y junctions, whose fixed point may not be known *a priori*.

Motivated by recent time-resolved experiments on 1D TLL wires [13,34], we study the propagation of a wave-packet incident from a FL lead in wire 1, in Fig. 3. Note that the results depicted in Fig. 3(a) are similar to the results for reflected current in type-I geometry for a 1D TLL wire, reported in Ref. [13]. Our results generalize the recent results of Ref. [34], for arbitrary-shaped wave-packet propagation in a single TLL wire to the case of multiwire junctions.

C. The DC limit

In the linear response regime, the dc conductivity of the Y junction is different if the TLL wires are connected to FL leads and if the TLL wires extend to infinity. This is well known for the case of a single TLL wire, whose linear dc conductance is e^2/h when connected to FL leads and is ge^2/h for an infinite TLL wire [38].

To obtain the dc conductivity for a Y junction connected to FL leads, from our ac results, we note that in the dc limit, i.e., as $\omega \to 0$ (or as $k \to 0$), for both classes of fixed points we have

$$\lim_{\omega\to 0} \mathbb{S} = \mathbb{M}. \tag{42}$$

This implies $I_i^{\rm out} = \sum_j \mathbb{M}_{ij} I_j^{\rm in}$, where we have defined $I_i^{\rm in(out)}$ to be the current flowing towards (away from) the junction in the TLL wire i. Further if V_j is the voltage applied in the FL lead connected to wire j, then the incoming current (per spin) is related to it by $I_i^{\rm in} = \sum_j (e^2/h)\delta_{ij} V_j$. Now using the definition of the junction conductance $\mathbb{G}$, which relates the net current flowing towards the junction to the external voltages, i.e., $I_i \equiv I_i^{\rm in} - I_i^{\rm out} = \sum_j \mathbb{G}_{ij} V_j$, we obtain the dc conductance matrix (per spin orientation) to be

$$\mathbb{G} = (e^2/h)(\mathbb{I} - \mathbb{M}). \tag{43}$$

For a Y junction with TLL leads extending to infinity, the voltage applied in the LL lead of wire j is related to the incoming current by $I_i^{\rm in} = \sum_j (ge^2/h)\delta_{ij} V_j$, and the current splitting matrix at the junction is $\tilde{\mathbb{M}}$. Thus the conductance matrix (per spin) is given by

$$\mathbb{G} = (ge^2/h)(\mathbb{I} - \tilde{\mathbb{M}}). \tag{44}$$

As a check of Eqs. (43) and (44), we note that they are consistent with the conductance of several fixed points reported in Ref. [19] using the Kubo formula and other methods. We emphasize here that the dc conductivity for a junction of finite-length TLL wires connected to FL leads does not carry any signature of interactions and charge fractionalization events in the system. In contrast, the ac conductivity depends on the *e-e* interactions as well as the length of each wire.

In the next section, we consider a Y junction of infinite-length TLL wires [see Fig. 1(b)], with pointlike tunneling impurities at the junction, and calculate the "tunneling" current and quantum noise at the junction.

IV. TUNNELING CURRENT AND TUNNELING NOISE AT THE JUNCTION

We now consider the effect of pointlike charge-conserving tunneling operators between infinite TLL wires, at the junction ($x = 0$), and study the tunneling current and low-frequency quantum noise arising due to these. Note that each of the boundary conditions at the junction characterized by θ corresponds to a scale invariant boundary condition, or a RG fixed point, of the bosonic field theory. The knowledge of $\mathbb{M}$ at each θ thus completely specifies all the reflection and transmission amplitudes at the level of the Hamiltonian for the Y junction—see Ref. [19]. Additional small tunneling (boundary operators) between wires may be treated as a small variation of the amplitudes. If all of the tunneling operators at the junction are irrelevant in a RG sense, then the fixed point is stable; otherwise, switching on of relevant tunneling operators around any fixed point makes the junction "flow" to another fixed point on changing length and energy scales in the system. In our case, a tunneling operator is relevant (irrelevant) if the boundary scaling dimension of the tunneling operators is less than (greater than) unity, i.e., $d_0 < 1$ ($d_0 > 1$). However, we emphasize that as long as the wire length is not very large (as compared to the other length scales set by the temperature or the external voltages), such that the RG flow does not take one far away from the fixed point (either stable or unstable), the calculations described in this section are still valid for all fixed points. A similar setup was used in Ref. [29] to study rectification in a Y junction of TLL wires, which was found to be strongest for junctions violating TRS and for strongly coupled junctions.

We consider very narrow (pointlike) tunneling barriers, so that the time duration of the tunneling event is much smaller than the time duration between two successive tunneling events. Such discrete tunneling events lead to the so-called shot noise, whose spectrum carries the signature of correlations between different tunneling events. In addition, we also have different voltages in different leads. This leads to the so-called Josephson noise, which arises from the quantum interference of the wave functions, on different sides of the tunneling impurity (different wires in our case), and it may lead to a divergence in the noise spectrum at frequency $\omega = qV_{\rm eff}/h$, where $V_{\rm eff}$ is the effective voltage difference that the tunneling operator is subjected to [32]. In what follows, we derive the tunneling noise at the junction from a perturbative calculation, which gives both the shot-noise and Josephson-noise contributions.

In a clean junction (no tunneling "impurity"), the current in wire i is given by $I_i = \mathbb{G}_{ij} V_j$, where $\mathbb{G}$ is given by Eq. (44) for a Y junction with infinite TLL wires. The switching on of the tunneling operators ($\psi^\dagger_{i\rm O}\psi_{j\rm I}$) in the vicinity ($x_i \leqslant 1/k_{\rm F}$) of the Y junction, which is tuned to be at a particular fixed point, leads to an additional tunneling current δI_i, such that $I_i^{\rm total} = I_i + \delta I_i$. If the tunneling Hamiltonian is expressed as

$$H_{\rm tunn} = \gamma \psi_{i\rm O}(0,t)^\dagger \psi_{j\rm I}(0,t) + \text{H.c.}, \tag{45}$$

then the tunneling current operator ($\delta\hat{I}_i$) is defined by

$$\delta\hat{I}_i(t) = q\frac{d\hat{\rho}_{i\rm O}}{dt} = -iq\hbar^{-1}[\hat{\rho}_{i\rm O}, \hat{H}_{\rm tunn}] = iq\gamma\hbar^{-1}[\psi^\dagger_{i\rm O}\psi_{j\rm I} - \text{H.c.}]. \tag{46}$$

It can be calculated at any time t from the following expression:

$$\langle\delta\hat{I}_i\rangle = \langle 0|S(-\infty;t)\delta\hat{I}_i(t)S(t;-\infty)|0\rangle, \tag{47}$$

where $|0\rangle$ denotes the ground state of the unperturbed system, i.e., the initial state at $t \to -\infty$. Here, S is the scattering matrix arising due to the tunneling impurities, and it is given by

$$S(t;-\infty) = S^\dagger(-\infty;t) = \mathcal{T}e^{-i\hbar^{-1}\int_{-\infty}^{t}\hat{H}_{\rm tunn}(t')dt'}, \tag{48}$$

where $\mathcal{T}$ denotes the time-ordering operator. Using the notation $\hat{B}_{ij}(x,t) \equiv \psi^\dagger_{i\rm O}\psi_{j\rm I}$ for the tunneling operator, and expressing the fermionic operators in terms of bosonic fields using Eq. (1), we get

$$\hat{B}_{ij}(x,t) = \frac{1}{2\pi\alpha}F^\dagger_{i\rm O}F_{j\rm I}e^{i(2\pi/L)(N_{i\rm O}-N_{j\rm I})vt}e^{-i\phi_{j\rm I}(x,t)}e^{-i\phi_{i\rm O}(x,t)}. \tag{49}$$

The tunneling current, in terms of the tunneling operator, is $\delta\hat{I}_i(t) = iq\gamma\hbar^{-1}[\hat{B}_{ij}(t) - \text{H.c.}]$, while the scattering matrix is given by $S(t,-\infty) = 1 - i\hbar^{-1}\gamma\int_{-\infty}^{t}dt'[\hat{B}_{ij}(t') + \text{H.c.}]$, up to first order in the tunneling amplitude γ. Thus the expectation value of the tunneling current operator, up to second order in γ, is given by

$$\delta I_i = \frac{q\gamma^2}{\hbar^2}\int_{-\infty}^{t}dt'\langle 0|[\hat{B}^\dagger_{ij}(t)B_{ij}(t') - \hat{B}_{ij}(t')\hat{B}^\dagger_{ij}(t)] + \text{H.c.}|0\rangle. \tag{50}$$

The symmetrized noise is given by the Fourier transform of the current-current correlator,

$$S(\omega) = \int_{-\infty}^{\infty}dt e^{-i\omega t}\langle\delta\hat{I}_i(t)\delta\hat{I}_i(0) + \delta\hat{I}_i(0)\delta\hat{I}_i(t)\rangle, \tag{51}$$

and up to second order in γ, we obtain

$$S(\omega) = \frac{q^2\gamma^2}{\hbar^2}\int_{-\infty}^{\infty}dt e^{-i\omega t} \times \langle 0|[\hat{B}_{ij}(t)B^\dagger_{ij}(0) + \hat{B}_{ij}(t)\hat{B}^\dagger_{ij}(0)] + \text{H.c.}|0\rangle. \tag{52}$$

To obtain the final expressions for the tunneling current and for the symmetrized quantum noise, we need the ground-state expectation values of operators, such as $\mathcal{O} \equiv \hat{B}_{ij}(x,t)\hat{B}^\dagger_{ij}(x',t')$. Following a standard procedure [5], at zero temperature (T), these are given by

$$\langle 0|\mathcal{O}|0\rangle = \frac{\alpha^{2d_0}}{4\pi^2\alpha^2}\frac{e^{i\frac{2\pi}{L}\langle 0|N_{i\rm O}-N_{j\rm I}|0\rangle v(t-t')}}{\{(x-x')^2 - [v(t-t') - i\alpha]^2\}^{d_0}}, \tag{53}$$

where d_0 is the boundary scaling dimension of the tunneling operator involved, i.e., $\hat{B}_{ij} = \psi^\dagger_{i\rm O}\psi_{j\rm I}$. For all possible tunneling operators, d_0 is tabulated in Table I for both the $\mathbb{M}_1$ and $\mathbb{M}_2$ class of fixed points [26]. In addition, we also have terms such as $N_{i\rm O} - N_{j\rm I}$ in the exponential whose expectation values depend on the external chemical potentials μ_i (or voltages V_i) applied on each wire in the grand canonical ensemble picture. The outgoing $N_{i\rm O}$ are related by the current splitting matrix $\mathbb{M}$ to the incoming $N_{i\rm I}$, which are in turn related to the external reservoir voltages. Thus we have

$$N_{i\rm O} = \sum_p \mathbb{M}_{ip}N_{p\rm I} \quad \text{and} \quad \frac{hv}{L}\langle N_{i\rm I}\rangle = \mu_i = qV_i. \tag{54}$$

TABLE I. Scaling dimensions of various tunneling operators for both $\mathbb{M}_1$ and $\mathbb{M}_2$ classes of fixed points.

Operators ($\mathbb{M}_1$ class)	Scaling dimension (d_0)
$\psi^\dagger_{i\mathrm{O}}\psi_{i\mathrm{I}}$	$\frac{4g(1-\cos\theta)}{3[g^2+(g^2-1)\cos\theta+1]}$
$\psi^\dagger_{2\mathrm{O}}\psi_{1\mathrm{I}},\psi^\dagger_{3\mathrm{O}}\psi_{2\mathrm{I}},\psi^\dagger_{1\mathrm{O}}\psi_{3\mathrm{I}}$	$\frac{2g(\cos\theta+\sqrt{3}\sin\theta+2)}{3[g^2+(g^2-1)\cos\theta+1]}$
$\psi^\dagger_{1\mathrm{O}}\psi_{2\mathrm{I}},\psi^\dagger_{2\mathrm{O}}\psi_{3\mathrm{I}},\psi^\dagger_{3\mathrm{O}}\psi_{1\mathrm{I}}$	$\frac{2g(\cos\theta-\sqrt{3}\sin\theta+2)}{3[g^2+(g^2-1)\cos\theta+1]}$
Operators ($\mathbb{M}_2$ class)	Scaling dimension (d_0)
$\psi^\dagger_{1\mathrm{O}}\psi_{1\mathrm{I}}$	$\frac{1}{3}g(2+\cos\theta-\sqrt{3}\sin\theta)$
$\psi^\dagger_{2\mathrm{O}}\psi_{2\mathrm{I}}$	$\frac{1}{3}g(2+\cos\theta+\sqrt{3}\sin\theta)$
$\psi^\dagger_{3\mathrm{O}}\psi_{3\mathrm{I}}$	$\frac{2}{3}g(1-\cos\theta)$
$\psi^\dagger_{1\mathrm{O}}\psi_{2\mathrm{I}},\psi^\dagger_{2\mathrm{O}}\psi_{1\mathrm{I}}$	$\frac{3+g^2}{6g}(1-\cos\theta)$
$\psi^\dagger_{2\mathrm{O}}\psi_{3\mathrm{I}},\psi^\dagger_{3\mathrm{O}}\psi_{2\mathrm{I}}$	$\frac{3+g^2}{12g}(2+\cos\theta-\sqrt{3}\sin\theta)$
$\psi^\dagger_{3\mathrm{O}}\psi_{1\mathrm{I}},\psi^\dagger_{1\mathrm{O}}\psi_{3\mathrm{I}}$	$\frac{3+g^2}{12g}(2+\cos\theta+\sqrt{3}\sin\theta)$

The expectation value of $\langle N_{i\mathrm{O}}-N_{j\mathrm{I}}\rangle$ now defines a new frequency scale which is related to external voltages by

$$\omega_0 \equiv \frac{2\pi v}{L}\langle N_{i\mathrm{O}}-N_{j\mathrm{I}}\rangle = h^{-1}q\left(\sum_p(\mathbb{M}_{ip}V_p)-V_j\right), \quad (55)$$

where j and p are wire indices. Physically, $\hbar\omega_0$ is the effective voltage difference that the tunneling operator "feels" (is subjected to) for an electron incoming in lead j and finally outgoing in lead i.

We now proceed to calculate the tunneling current by substituting Eqs. (55) and (53) in Eq. (50). A straightforward calculation, using the integral

$$I_\pm = \int_{-\infty}^{\infty}dt'\frac{e^{\pm i\omega_0 t'}}{\left(\frac{\alpha}{v}-it'\right)^{2d_0}} = \frac{2\pi|\omega_0|^{2d_0-1}}{\Gamma(2d_0)}e^{-\frac{\alpha|\omega_0|}{v}}\theta(\mp\omega_0) \quad (56)$$

gives

$$\delta I_i = q\frac{2\pi\gamma^2}{h^2\alpha^2}\frac{1}{\Gamma(2d_0)}\left(\frac{\alpha}{v}\right)^{2d_0}|\omega_0|^{2d_0-1}\mathrm{sign}(\omega_0). \quad (57)$$

Here, $\Gamma(2d_0)$ appearing in the denominator is the gamma function. The scaling dimension d_0, in general, depends on the strength of interactions and the fixed point (θ) that the junction is tuned to. It is tabulated in Table I, and a contour plot of d_0 in the (θ,g) parameter space is presented in Fig. 4. For the case of a "noninteracting" junction, i.e., $d_0\to 1$ (which is equivalent to the case of $g\to 1$ in a single-wire scenario), $\delta I_i|_{d_0\to 1} = q\frac{2\pi\gamma^2}{h^2v^2}\omega_0$. In the limiting case of $d_0\to 1/2$ (which is equivalent to the case of $g\to 1/2$ in the single-wire scenario), we have $\delta I_i|_{d_0\to\frac{1}{2}} = q\frac{2\pi\gamma^2}{h^2\alpha v}\mathrm{sign}(\omega_0)$.

To relate it to an earlier work, let us consider the fixed point $\theta=0$ of the $\mathbb{M}_2$ class, i.e., $[a,b,c]=[1,0,0]$, which represents the specific case of wires 1 and 2 being directly connected and wire 3 being completely disconnected. Now consider a tunneling operator $\psi^\dagger_{2\mathrm{O}}\psi_{2\mathrm{I}}$, for which $\omega_0 = h^{-1}q(V_1-V_2)$ and $d_0=g$. The tunneling current in this case is given by

$$\delta I_i = q\frac{2\pi\gamma^2}{h^2\alpha^2}\frac{1}{\Gamma(2g)}\left(\frac{\alpha}{v}\right)^{2g}|h^{-1}q(V_1-V_2)|^{2g-1}, \quad (58)$$

which has earlier been reported in the context of current enhancement by a tunneling impurity in Ref. [39], and as a limiting case of two or more impurity scattering in TLL wires in Refs. [40,41].

Equation (57) can be generalized to finite temperatures by using the following transformation [32]:

$$I_\pm = \int_{-\infty}^{\infty}dt'\frac{e^{\pm i\omega_0 t'}}{\left(\frac{\alpha}{v}-it'\right)^{2d_0}} \to e^{i\pi d_0}\int_{-\infty}^{\infty}dt'\frac{e^{\pm i\omega_0 t'}}{\left|\frac{\sinh(\pi Tt')}{\pi T}\right|^{2d_0}}, \quad (59)$$

which gives

$$I_\pm(T) = 2(\pi T)^{2d_0-1}B\left(d_0+\frac{i\omega_0}{2\pi T},d_0-\frac{i\omega_0}{2\pi T}\right)e^{\pm\frac{\omega_0}{2T}}, \quad (60)$$

where T denotes the temperature in units of $k_B/\hbar$, with k_B being the Boltzman constant, and $B(x,y)=B(y,x)$ is the β function. The β function can also be written in terms of the Γ function: $B(x,y)=\Gamma(x)\Gamma(y)/\Gamma(x+y)$. The tunneling current at finite $T\leqslant\hbar v/\alpha$ is now given by

$$\delta I_i(T) = q\frac{4\gamma^2}{h^2\alpha^2}\left(\frac{\alpha}{v}\right)^{2d_0}(\pi T)^{2d_0-1} \times B\left(d_0+\frac{i\omega_0}{2\pi T},d_0-\frac{i\omega_0}{2\pi T}\right)\sinh\left(\frac{\omega_0}{2T}\right). \quad (61)$$

In the limiting case of $d_0\to 1$, we can use the identity $\Gamma(1+ix)\Gamma(1-ix)=\pi x/\sinh(\pi x)$ to obtain $\delta I_i(T)|_{d_0\to 1} = q\frac{2\pi\gamma^2}{h^2v^2}\omega_0$, independent of the temperature. For the case of $d_0\to 1/2$, one can use the identity $\Gamma(1/2+ix)\Gamma(1/2-ix)=\pi/\cosh(\pi x)$ to get $\delta I_i(T)|_{d_0\to\frac{1}{2}} = q\frac{4\pi\gamma^2\alpha}{h^2v}\tanh[\omega_0/(2T)]$.

The symmetrized quantum noise, up to second order in the tunneling strength γ, can also be calculated in a similar fashion and is given by

$$S(\omega) = q^2\frac{2\pi\gamma^2}{h^2\alpha^2}\frac{1}{\Gamma(2d_0)}\left(\frac{\alpha}{v}\right)^{2d_0} \times(|\omega-\omega_0|^{2d_0-1}+|\omega+\omega_0|^{2d_0-1}). \quad (62)$$

It can be expressed in terms of the tunneling current as

$$S(\omega) = q\delta I_i(|1-\omega/\omega_0|^{2d_0-1}+|1+\omega/\omega_0|^{2d_0-1}). \quad (63)$$

As a check of our calculations, we note that for the specific case of $\theta=0$, discussed in the previous paragraph, Eq. (62) of our paper reproduces Eq. (17) of Ref. [32], in which the authors studied the perturbative noise for a small point impurity in an otherwise clean TLL. In the limit $|\omega/\omega_0|\to 0$ or at small frequencies, $S(\omega)\approx 2q\delta I_i$ independent of the interaction parameter, which is the typical Schottky's shot-noise result. It corresponds to the uncorrelated arrival of particles at the tunnel barrier, whereby the time interval between arrival times is described by a Poissonian distribution. In the opposite limit of $|\omega_0/\omega|\to 0$, we get $S(\omega)\approx 2q\delta I_i|\omega/\omega_0|$, consistent with results for noninteracting electrons [32]. In the limiting case of $d_0\to 1$, for low frequencies ($\omega<\omega_0$), we have $S(\omega)|_{d_0\to 1} = 2q\delta I_i$, while for high frequencies ($\omega>\omega_0$), we have $S(\omega) = 2q\delta I_i\frac{\omega}{\omega_0}$, giving a linear dependence on the frequency. Note that the high-frequency limit of the noise spectrum for $d_0\to 1$ is primarily determined by zero point fluctuations and is

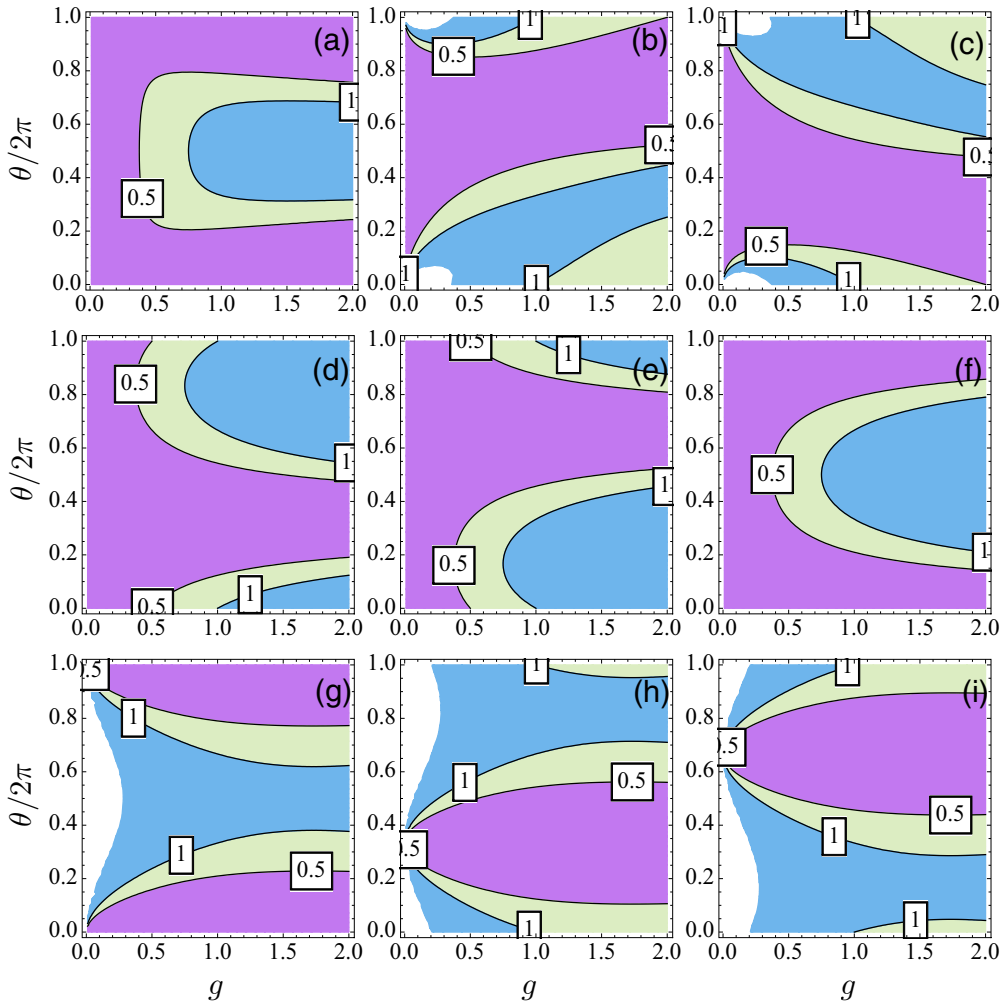

FIG. 4. (Color online) The scaling dimension for various tunneling operators. (a)–(c) The operators $\psi^\dagger_{i\mathrm{O}}\psi_{i\mathrm{I}}$, $\psi^\dagger_{1\mathrm{O}}\psi_{2\mathrm{I}}$, and $\psi^\dagger_{2\mathrm{O}}\psi_{1\mathrm{I}}$, respectively, for the $\mathbb{M}_1$ class of fixed points (as they appear in Table I). (d)–(i) The scaling dimensions of various tunneling operators as they appear in Table I, for the $\mathbb{M}_2$ class of fixed points. In all panels, the purple region has $d_0 < 1/2$, the green region represents $1/2 < d_0 < 1$, and the blue region has $d_0 > 1$. Both the backscattering current and the quantum noise show diverging behavior for $d_0 < 1/2$, i.e., in the (θ, g) parameter space represented in purple. Also note that the tunneling operators become relevant in the region $d_0 < 1$, i.e., purple and green regions, and will make the junction "flow" to another fixed point.

independent of the applied voltages, as expected [42]. In the limit $d_0 \to 1/2$, we obtain $S(\omega)|_{d_0\to\frac{1}{2}} = 2q\delta I_i$.

The noise power spectrum in Eq. (62) can also be generalized to include finite-temperature effects. Using the mapping of Eq. (59), we obtain the finite-temperature symmetrized noise to be

$$S(\omega) = q^2\frac{4\gamma^2}{h^2\alpha^2}\left(\frac{\alpha}{v}\right)^{2d_0}(\pi T)^{2d_0-1}[f(\omega+\omega_0)+f(\omega-\omega_0)], \tag{64}$$

where

$$f(x) = \cosh\left[\frac{x}{2T}\right]B\left(d_0+\frac{ix}{2\pi T},d_0-\frac{ix}{2\pi T}\right). \tag{65}$$

Note that finite temperature smears the singularities of the noise power spectrum. The zero-frequency limit of Eq. (64) gives

$$S(\omega\to 0) = 2q\delta I_i(T)\coth\left[\frac{\omega_0}{2T}\right], \tag{66}$$

which is the equivalent of the equilibrium Johnson-Nyquist noise for a Y junction. For the case of $d_0 \to 1$, we get $S(\omega,T)|_{d_0\to 1} = q\frac{2\pi\gamma^2}{h^2v^2}[h(\omega+\omega_0)+h(\omega-\omega_0)]$, where $h(x) = x\coth[x/(2T)]$. For $d_0 \to 1/2$, we have $S(\omega,T)|_{d_0\to 1/2} = 2q\delta I_i(T)\coth[\omega_0/(2T)]$.

We plot the ratio $\delta I_1/\delta I_1(d_0 = 1)$ versus ω_0 in Fig. 5(a), for the backscattering operator $\psi^\dagger_{1\mathrm{O}}\psi_{1\mathrm{I}}$ when the junction is tuned to be at the χ_+ fixed point. The divergence of this ratio whenever $2d_0 - 2 < 0$ is evident. The ratio $S(\omega)/2q\delta I_1$ is plotted in Fig. 5(b). This ratio diverges whenever $2d_0 - 1 < 0$.

An important difference in the three-wire case compared to the two-wire case is that both ω_0 and d_0, i.e., the frequency of divergence in $S(\omega)$ as well as the power law of divergence, are, in general, complicated functions of the boundary conditions at the junction ($\mathbb{M}$) and the *e-e* interaction strength. Note that the noise diverges as $\omega \to \pm\omega_0$ when $d_0 < 1/2$. We believe that this divergence is not a limitation of our γ^2 perturbation theory and it will persist even if we go to higher orders in γ, as in the case of a "tunneling" impurity in a single TLL

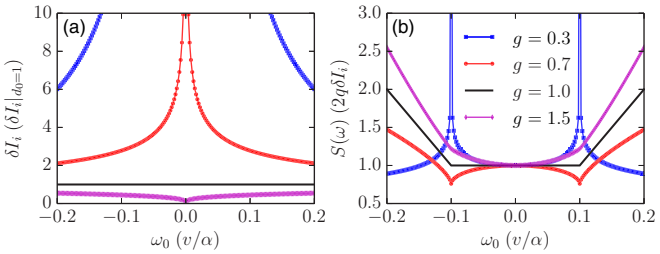

FIG. 5. (Color online) The (a) tunneling current and (b) quantum noise in wire 1, as a function of ω_0, for different values of the interaction strength. The junction is tuned to the "chiral" fixed point (χ_+), i.e., $\theta = 4\pi/3$ in the $\mathbb{M}_1$ class, and the tunneling operator is chosen to be the backscattering operator $\psi^\dagger_{\mathrm{O1}}\psi_{\mathrm{I1}}$. The scaling dimension of $\psi^\dagger_{\mathrm{O1}}\psi_{\mathrm{I1}}$ at the χ_+ fixed point for $g = (0.3, 0.7, 1, 1.5)$, which corresponds to the lines represented by the blue square, red circle, black solid, and magenta diamond markers, respectively, in both panels, is given by $d_0 = (0.39, 0.84, 1, 1.14)$. We have chosen $\omega = 0.1\alpha/v$ for (b).

wire [32]. However, this divergence is a limitation of our low-energy theory, and in a realistic experimental scenario it should be regularized by the highest relevant energy scale (e.g., temperature or the maximum external voltage) . This is usually achieved by replacing the ultraviolet energy cutoff $\hbar v/\alpha$ by $k_B T$ or $\max[V_1, V_2, V_3]$.

Finally, we note that the results of this section are valid for an electronic Y junction as well as for a quasiparticle junction formed from quantum Hall (QH) edge states. The substitution $q \to e$ accounts for electron tunneling and $q \to \nu e$ takes care of quasiparticle tunneling in QH edge states, where e denotes the electron charge and ν is the QH filling fraction.

V. SUMMARY AND CONCLUSIONS

In this paper, we investigated the ac conductivity of a Y junction formed from finite-length TLL wires connected to FL reservoirs, based on the plasmon scattering approach, for injected charge pulses of arbitrary shapes. This formalism gives the full spatiotemporal profile of the charge wave packet in all the wires, and is therefore very useful for analyzing time-resolved transport experiments in TLL wires [13,34] and their junctions. We find that unlike the dc conductivity of a "clean" junction, the ac conductivity depends on the strength of the e-e interactions and the length of the wire. Consequently, it carries signatures of charge fractionalization at the TLL-FL interface as well as at the junction. The ac conductivity also displays an oscillatory behavior as a function of the frequency of the incoming pulse, with the periodicity of $\pi\tilde{v}/L$ for the time-reversal symmetric junctions, i.e., junctions characterized by $\mathbb{M}_2$ class of fixed points, and with a period of $2\pi\tilde{v}/L$ for junctions which break time-reversal symmetry, i.e., those characterized by the $\mathbb{M}_1$ class of fixed points. The limitation of our calculation is that it is valid only for low ac frequencies which do not breach the linearization regime of each TLL wire, i.e., $\omega < v/\alpha$.

Additionally, we consider pointlike tunneling impurities at the junction of infinite TLL wires, and find the corresponding tunneling current and quantum noise spectrum. We explicitly show that the correlations arising from strong e-e interactions in TLL wires give rise to singularities in the noise spectrum (calculated up to second order in γ), as a function of the frequency or the applied voltage. The divergence in the noise spectrum for some specific frequencies will possibly persist to even higher orders in γ, and is an artifact of the effective low-energy TLL Hamiltonian that we are using. In any realistic experimental scenario, the high-energy or ultraviolet cutoff α^{-1} will get replaced by the other energy scales such as the temperature or the maximum applied voltage, which would cut off the divergences. Another important aspect to consider is that these calculations are valid only in the "tunneling" limit, until γ does not flow (in a RG sense) beyond the TLL bandwidth [43], i.e., $\gamma^2 < (\alpha(|\omega \pm \omega_0|/v)^{1-2d_0}$. Note that similar effects have been reported in a tunneling scenario in a two-wire junction [32,39], where such divergences occur at very strong e-e interaction strength of $g < 1/2$, which is a difficult regime to probe experimentally. However, the three-wire junction offers the possibility of being tuned (by means of nanogates applied in the vicinity the junction) to various fixed points, where these enhancements in the tunneling current and divergence of the quantum noise can also occur in a very wide regime of g, including attractive e-e interaction strengths—see Fig. 4.

We firmly believe that both of these studies, i.e., the effects of pulse propagation in a Y junction and "backscattering" by tunneling impurities at the junction, will be very useful for interpreting time-resolved experiments [13,34] in multiwire junctions of interacting electrons, and in the design and fabrication of quantum circuitry in the future. Experimentally, TLL wire Y junctions may be fabricated using carefully patterned 1D wires in a two-dimensional electron gas, and tuned to various fixed points by means of nanogates applied near the junction. Another possibility is an "island" setup proposed in Ref. [21], formed from quantum Hall edge states, which may be more feasible. In this case, the tunneling operators can be controlled by means of gate voltage operated constrictions in the central region of the island.

ACKNOWLEDGMENTS

We thank Diptiman Sen for stimulating discussions and for carefully reading the paper. We gratefully acknowledge funding from the INSPIRE Faculty Award by DST (Government of India) and from the Faculty Initiation Grant by IIT Kanpur, India.

[1] S. Tomonaga, Prog. Theor. Phys. **5**, 544 (1950).
[2] J. M. Luttinger, J. Math. Phys. **4**, 1154 (1963).
[3] D. C. Mattis and E. H. Lieb, J. Math. Phys. **6**, 304 (1965).
[4] F. D. Haldane, J. Phys. C **14**, 2585 (1981).
[5] J. V. Delft and H. Schoeller, Ann. Phys. **7**, 225 (1998); S. Rao and D. Sen, in *Field Theories in Condensed Matter Physics*, edited by S. Rao (Hindustan, New Delhi, 2001).

[6] T. Giamarchi, *Quantum Physics in One Dimension* (Oxford University Press, Oxford, 2004).

[7] D. Pines and P. Nozieres, *The Theory of Quantum Liquids* (Benjamin, New York, 1966); G. F. Giuliani and G. Vignale, *Quantum Theory of the Electron Liquid* (Cambridge University Press, Cambridge, 2005).

[8] O. M. Auslaender, H. Steinberg, A. Yacoby, Y. Tserkovnyak, B. I. Halperin, K. W. Baldwin, L. N. Pfeiffer, and K. W. West, Science **308**, 88 (2005).

[9] Y. Jompol, C. J. B. Ford, J. P. Griffiths, I. Farrer, G. A. C. Jones, D. Anderson, D. A. Ritchie, T. W. Silk, and A. J. Schofield, Science **325**, 597 (2009).

[10] I. Safi and H. J. Schulz, Phys. Rev. B **52**, R17040 (1995).

[11] K.-V. Pham, M. Gabay, and P. Lederer, Eur. Phys. J. B **9**, 573 (1999); Phys. Rev. B **61**, 16397 (2000).

[12] H. Steinberg, G. Barak, A. Yacoby, L. N. Pfeiffer, K. W. West, B. I. Halperin, and K. Le Hur, Nat. Phys. **4**, 116 (2008).

[13] H. Kamata, N. Kumada, M. Hashisaka, K. Muraki, and T. Fujisawa, Nat. Nanotechnol. **9**, 177 (2014).

[14] M. S. Fuhrer, J. Nygard, L. Shih, M. Forero, Y.-G. Yoon, M. S. C. Mazzoni, H. J. Choi, J. Ihm, S. G. Louie, A. Zettl, and P. L. McEuen, Science **288**, 494 (2000).

[15] M. Terrones, F. Banhart, N. Grobert, J.-C. Charlier, H. Terrones, and P. M. Ajayan, Phys. Rev. Lett. **89**, 075505 (2002).

[16] C. Nayak, M. P. A. Fisher, A. W. W. Ludwig, and H. H. Lin, Phys. Rev. B **59**, 15694 (1999).

[17] S. Lal, S. Rao, and D. Sen, Phys. Rev. B **66**, 165327 (2002); S. Das, S. Rao, and D. Sen, *ibid.* **70**, 085318 (2004).

[18] S. Chen, B. Trauzettel, and R. Egger, Phys. Rev. Lett. **89**, 226404 (2002); R. Egger, B. Trauzettel, S. Chen, and F. Siano, New J. Phys. **5**, 117 (2003).

[19] C. Chamon, M. Oshikawa, and I. Affleck, Phys. Rev. Lett. **91**, 206403 (2003); M. Oshikawa, C. Chamon, and I. Affleck, J. Stat. Mech. (2006) P02008.

[20] X. Barnabé-Thériault, A. Sedeki, V. Meden, and K. Schönhammer, Phys. Rev. B **71**, 205327 (2005); Phys. Rev. Lett. **94**, 136405 (2005).

[21] S. Das, S. Rao, and D. Sen, Phys. Rev. B **74**, 045322 (2006).

[22] D. Giuliano and P. Sodano, Nucl. Phys. B **811**, 395 (2009); New J. Phys. **10**, 093023 (2008).

[23] B. Bellazzini, M. Burrello, M. Mintchev, and P. Sorba, *Proceedings of Symposia in Pure Mathematics*, edited by P. Exner, J. P. Keating, P. Kuchment, T. Sunada, and A. Teplyaev, Vol. 77 (American Mathematical Society, Providence, RI, 2008), p. 639; B. Bellazzini, P. Calabrese, and M. Mintchev, Phys. Rev. B **79**, 085122 (2009).

[24] C.-Y. Hou and C. Chamon, Phys. Rev. B **77**, 155422 (2008).

[25] S. Das and S. Rao, Phys. Rev. B **78**, 205421 (2008).

[26] A. Agarwal, S. Das, S. Rao, and D. Sen, Phys. Rev. Lett. **103**, 026401 (2009); **103**, 079903 (2009).

[27] A. Soori and D. Sen, Europhys. Lett. **93**, 57007 (2011); Phys. Rev. B **84**, 035422 (2011).

[28] A. Rahmani, C.-Y. Hou, A. Feiguin, C. Chamon, and I. Affleck, Phys. Rev. Lett. **105**, 226803 (2010); A. Rahmani, C.-Y. Hou, A. Feiguin, M. Oshikawa, C. Chamon, and I . Affleck, Phys. Rev. B **85**, 045120 (2012).

[29] C. Wang and D. E. Feldman, Phys. Rev. B **83**, 045302 (2011).

[30] C.-Y. Hou, A. Rahmani, A. E. Feiguin, and C. Chamon, Phys. Rev. B **86**, 075451 (2012).

[31] D. N. Aristov and P. Wölfle, Phys. Rev. B **86**, 035137 (2012); **88**, 075131 (2013).

[32] C. de C. Chamon, D. E. Freed, and X. G. Wen, Phys. Rev. B **51**, 2363 (1995).

[33] E. Berg, Y. Oreg, E.-A. Kim, and F. von Oppen, Phys. Rev. Lett. **102**, 236402 (2009).

[34] E. Perfetto, G. Stefanucci, H. Kamata, and T. Fujisawa, Phys. Rev. B **89**, 201413(R) (2014).

[35] S. Jezouin, M. Albert, F. D. Parmentier, A. Anthore, U. Gennser, A. Cavanna, I. Safi, and F. Pierre, Nat. Commun. **4**, 1802 (2013).

[36] A. Agarwal, S. Das, and D. Sen, Phys. Rev. B **81**, 035324 (2010).

[37] A. Agarwal and D. Sen, J. Phys.: Condens. Matter **21**, 375601 (2009); D. Sen and A. Agarwal, Phys. Rev. B **78**, 085430 (2008).

[38] D. L. Maslov and M. Stone, Phys. Rev. B **52**, R5539 (1995).

[39] D. E. Feldman and Y. Gefen, Phys. Rev. B **67**, 115337 (2003).

[40] D. Makogon, V. Juricic, and C. M. Smith, Phys. Rev. B **74**, 165334 (2006).

[41] A. Agarwal and D. Sen, Phys. Rev. B **76**, 035308 (2007).

[42] Y. M. Blanter and M. Büttiker, Phys. Rep. **336**, 1 (2000).

[43] C. L. Kane and M. P. A. Fisher, Phys. Rev. Lett. **68**, 1220 (1992); Phys. Rev. B **46**, 15233 (1992).